Acute spinal subdural hematoma: MR and CT findings with pathologic correlates.

M J Post, J L Becerra, P W Madsen, W Puckett, R M Quencer, R P Bunge and E M Sklar

AJNR Am J Neuroradiol 1994, 15 (10) 1895-1905
http://www.ajnr.org/content/15/10/1895

Acute Spinal Subdural Hematoma: MR and CT Findings with Pathologic Correlates

M. Judith Donovan Post, Jose L. Becerra, Parley W. Madsen, William Puckett, Robert M. Quencer, R. P. Bunge, and Evelyn M. L. Sklar

PURPOSE: To determine the MR and CT findings that characterize acute spinal subdural hematoma (ASSH). **METHODS:** The MR, CT, and clinical findings in three patients with surgically proved ASSH were reviewed and also correlated with the postmortem MR, CT, and cryomicrotome findings in three other patients, two with ASSH and one with an acute spinal epidural hematoma. **RESULTS:** Imaging findings in ASSH included: (*a*) hyperdense lesions on plain CT within the dural sac, distinct from the adjacent low-density epidural fat and silhouetted against the lower-density spinal cord and cauda equina, which it compressed; (*b*) lack of direct continuity with the adjacent osseous structures; (*c*) clumping, loculation, and streaking of blood within the dural sac on both MR and CT; and (*d*) an inhomogeneous and variable signal intensity to the ASSH on all MR pulse sequences, but, nevertheless, a striking low signal intensity on T2-weighted spin-echo or T2-weighted gradient-echo to a major part of the ASSH because of deoxyhemoglobin. Plain CT was most helpful in compartmentalizing the hematoma. **CONCLUSION:** When MR and plain CT are obtained as complementary studies, they provide characteristic findings that allow the prompt diagnosis of ASSH.

Index terms: Hematoma, spinal; Hematoma, subdural; Spine, computed tomography; Spine, magnetic resonance; Pediatric neuroradiology

AJNR Am J Neuroradiol 15:1895–1905, Nov 1994

Acute spinal subdural hematoma (ASSH) is an uncommonly recognized condition that if left untreated can result in severe irreversible neurologic deficits (1–7). Like acute spinal epidural hematomas, these ASSHs can expand rapidly and extend over many spinal segments, causing sudden spinal cord and/or cauda equina compression (1–19). Because rapid surgical decompression can reverse neurologic deficits or halt their progression, prompt recognition of this condition can affect patient outcome favorably. Despite the importance of early diagnosis, the imaging characteristics of ASSH, unlike acute spinal epidural hematoma (11–29), have not been well elucidated. Recent experience at our institution with three patients with surgically proved ASSH prompted us to review their clinical and imaging findings and correlate them with the postmortem magnetic resonance (MR) and computed tomographic (CT) scans and cryomicrotome data in three other patients with spinal hematomas to determine what imaging patterns are characteristic of this condition.

Received November 19, 1993; accepted after revision March 9, 1994.

Presented at the 31st Annual Meeting of the American Society of Neuroradiology, Vancouver, Canada, May 1993. Supported by grant I PO1 NS-28059-01 A1 from the National Institute of Neurological Disorders and Stroke and by the Miami Project to Cure Paralysis.

From the Departments of Radiology (Neuroradiology Section) (M.J.D.P., J.L.B., R.M.Q., E.M.L.S.) and Neurological Surgery (P.W.M.) and the Miami Project to Cure Paralysis (W.P., R.P.B.), University of Miami School of Medicine/Jackson Memorial Medical Center, Fla.

Address reprint requests to M. Judith Donovan Post, MD, Neuroradiology Section, MRI Center, 1115 NW 14th St, Miami, FL 33136.

AJNR 15:1895–1905, Nov 1994 0195-6108/94/1510–1895

Subjects and Methods

Postmortem material was obtained from three children who had sustained significant trauma from motor vehicle accidents or shaking episodes. They were either dead on arrival or died within 2 days of the injuries. Their vertebral columns with the spinal cords in situ were removed at autopsy and were placed immediately in 10% buffered formalin for 2 weeks and then stored in 0.01 mol/L phosphate buffer at 4°C. With a shoulder and cervical surface

coil, plain MR images were then acquired on a 1.5-T unit with a 3-mm section thickness and with T1- and T2-weighted images and T2-weighted gradient-echo MR sequences. Pulse parameters were as follows: (*a*) axial T1-weighted, 750/20/4 (repetition time/echo time/excitations), 90° flip angle; (*b*) sagittal T1-weighted, 500/20/4, 90° flip angle; (*c*) sagittal and coronal T2-weighted, 2000/80/2, 90° flip angle; (*d*) axial gradient-echo, 600/13/4, 20° flip angle; (*e*) sagittal gradient-echo, 500/13/4, 20° flip angle. Images were displayed on an image matrix of 192 or 256 × 256. CT scans were then obtained on these same specimens in the sagittal view with 1.5-mm-thick sections. Subsequently, the frozen vertebral columns with spinal cords in situ were prepared for sectioning on a Reichart-Jung Cryomacrocut (Leica, Heidelberg, Germany). They were oriented to be sectioned sagittally and photographed at approximately 1-mm intervals. Cryomicrotome findings were then correlated with the postmortem MR and CT results to determine the precise location and the imaging characteristics of the extravascular blood in the spinal canal and the relationship of the hematomas to the spinal cord and cauda equina.

In three hospitalized patients, plain CT scans with 3.0- to 5-mm-thick sections were done. Plain MR scans were then acquired within 6 to 36 hours of the CT. They were all done on a 1.5-T unit with a surface coil and 4.7- to 7-mm-thick sections. Pulse parameters were as follows: (*a*) axial T1-weighted, 800/16/1, 90° flip angle; (*b*) sagittal T1-weighted, 600/20/4, 90° flip angle; (*c*) sagittal proton-density and T2-weighted, 2382/20,80/2, 90° flip angle; (*d*) axial gradient-echo, 750–1000/18/1, 20° flip angle; (*e*) sagittal gradient-echo, 600/18/4, 20° flip angle. Field of view was 23 cm for axial and 30 cm for sagittal images. Images were displayed on a matrix of 200 to 220 × 256. These MR and CT scans were then reviewed and correlated with the surgical findings to ascertain in what spinal compartments the hematomas were residing, how extensive they were, how much neural compression they were associated with, and what signal characteristics they had on MR and what density they had on CT.

Results

The three hospitalized patients were two adults (ages 21 and 35 years) and one child (age 11), the latter leukemic. All three had abnormal clotting studies. In one of the adults, a gunshot-wound victim with a history of alcohol abuse and a long complicated hospital course, the coagulopathy was related to liver dysfunction. In the other adult, who had an encephalopathy, the patient was on anticoagulant therapy. Acute paraplegia developed in all three patients after multiple unsuccessful attempts at lumbar puncture (n = 2) or epidural anesthesia (n = 1). Imaging studies were initiated within 24 hours of symptom onset. All three underwent surgical evacuation of their iatrogenic ASSH, which as demonstrated on the imaging studies and documented at surgery were extensive in all three extending over 12 to 14 spinal levels and associated with spinal cord and cauda equina compression. Small amounts of subarachnoid hemorrhage and/or epidural blood were also found.

The postmortem cases were of three infants, all of whom died directly as the result of severe trauma. In two of these infants (both 8 months of age), the trauma resulted in severe injuries to the spine. The cervical spine was the site of injury in one and the thoracolumbar spine and coccyx the affected site in the other. The mechanism of injury was a motor vehicle accident in the first and child abuse with severe injury to the back, abdomen, and head in the second. After death, MR, CT, and cryomicrotome analysis in these two infants revealed sizeable acute spinal subdural hematomas extending over four to six spinal levels. In addition, spinal cord injury (consisting of cord severance in one and conus maceration in the other), vertebral body fractures (C-3 and C-7 in one and T-12 and the coccyx in the other), disk injuries, and small collections of epidural and subarachnoid blood were also present. In the third infant (age 5 months), also a victim of child abuse, no cord injury was present. Findings in this child with an injury caused by shaking included mild compression fractures of T-5 and T-8, disk injury (at T-7 to T-8), and a one-level small acute spinal posterior epidural hematoma (at T-6 to T-7), which was not associated with any cord compression.

Our imaging results in both the antemortem and postmortem cases of ASSH revealed the following findings. On plain CT the ASSH appeared as a hyperdense lesion within the dural sac distinct from the adjacent low-density epidural fat and osseous structures (Fig 1). Clumping, loculation, and streaking of blood within the dural sac were noted. Similarly, on MR, clumping, loculation, and occasionally streaking of blood were also noted within the dural sac (Fig 2) distinct from the adjacent bone and epidural fat, the latter hyperintense on T1-weighted images and hypointense on gradient-echo images. An inhomogeneous and variable signal intensity to the ASSH (depending on its exact age) was seen on all pulse sequences (Figs 3–5). On T1-weighted images the acute subdural blood

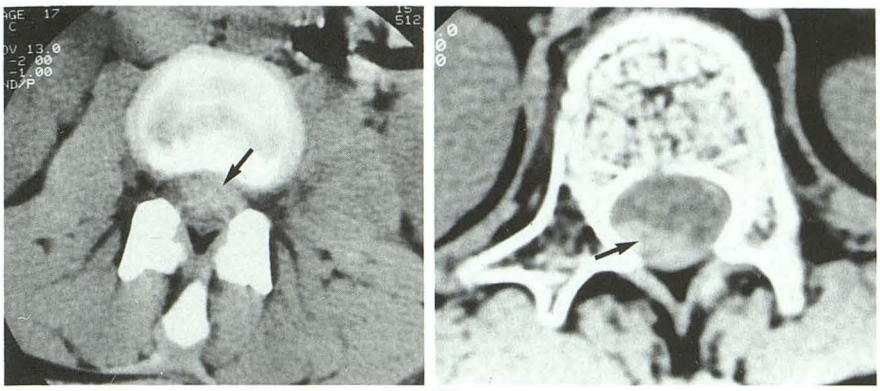

Fig 1. ASSHs: plain CT appearance. Plain CT scans in two patients with surgically proved ASSH show hyperdense lesions within the thecal sac (*arrows*), loculated predominantly to the ventral aspect of the spinal canal at L-3 in one patient (*A*) and to the dorsal aspect of the spinal canal at L-1 in the other (*B*).

appeared heterogeneous with isointense to slightly hyperintense and sometimes also hypointense signal. On T2-weighted or gradient-echo images the ASSH was characterized by areas of hypointensity, isointensity, and hyperintensity. Despite this heterogeneous signal, a striking low signal intensity was seen in a significant portion of the ASSH on T2-weighted or gradient-echo images and dominated the imaging findings (Figs 3C–E, 4B, and 5C).

To compare MR with CT in the cases of ASSH, plain CT more clearly compartmentalized the acute spinal hematomas in the subdural space (Fig 4), especially in cases in which the signal changes in the hematomas were inhomogeneous and in cases complicated by smaller amounts of blood in other compartments (eg, subarachnoid and epidural spaces). Fractures, although obvious on both imaging studies, were seen with greater anatomic clarity on CT. However, disk injury was more readily recognized on MR (Fig 5) because of the hyperintense signal abnormalities on both the T1-weighted and the T2-weighted or gradient-echo images. Neural damage was also more readily detected on MR. Spinal cord contusion was seen as areas of hyperintense signal on T2-weighted or gradient-echo images, which when complicated by hemorrhage also had areas of hypointensity. Spinal cord and cauda equina compression were also more clearly delineated on MR than on plain CT, especially on the axial T2-weighted or gradient-echo images.

Unlike the ASSHs, the epidural hematoma (found in one of the postmortem cases) appeared "capped" by the surrounding epidural fat. It was directly adjacent to the osseous structures and was not confined within the dural sac, but rather was located outside the sac in the extradural space.

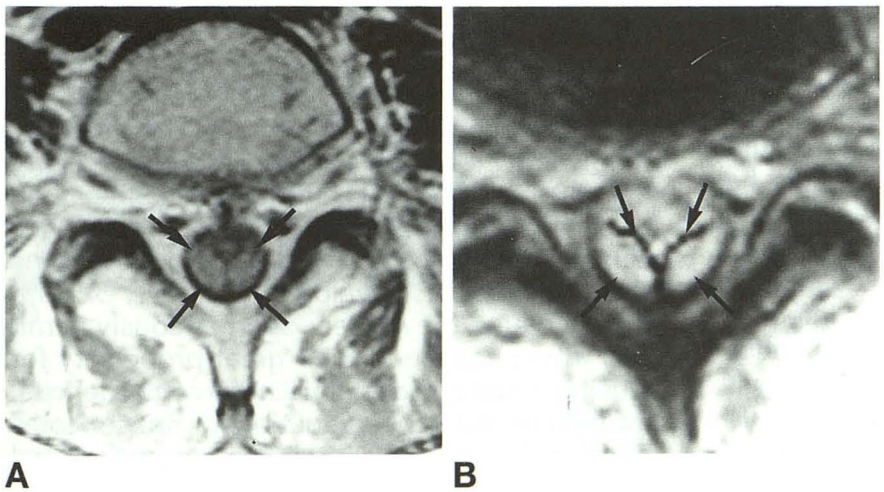

Fig 2. ASSHs: plain MR appearance. Plain MR at the L-5 level shows a loculated collection (*arrows*) within the thecal sac appearing *A*, isointense in signal to spinal cord on the T1-weighted image and *B*, heterogeneous on the gradient-echo image, with hyperintense signal centrally and hypointense signal peripherally. The anterior two *arrows* in *B* point to the deoxyhemoglobin at the peripheral medial margin of this collection. Notice that this bilobed collection is confined within the dural sac and does not diffuse freely within the thecal sac and is clearly separate from the adjacent epidural fat, which appears bright on the T1-weighted image and hypointense on the gradient-echo image. Notice also that this hematoma is compressing and displacing anteriorly the cerebrospinal fluid and cauda equina in the subarachnoid space. An ASSH was found and evacuated at surgery.

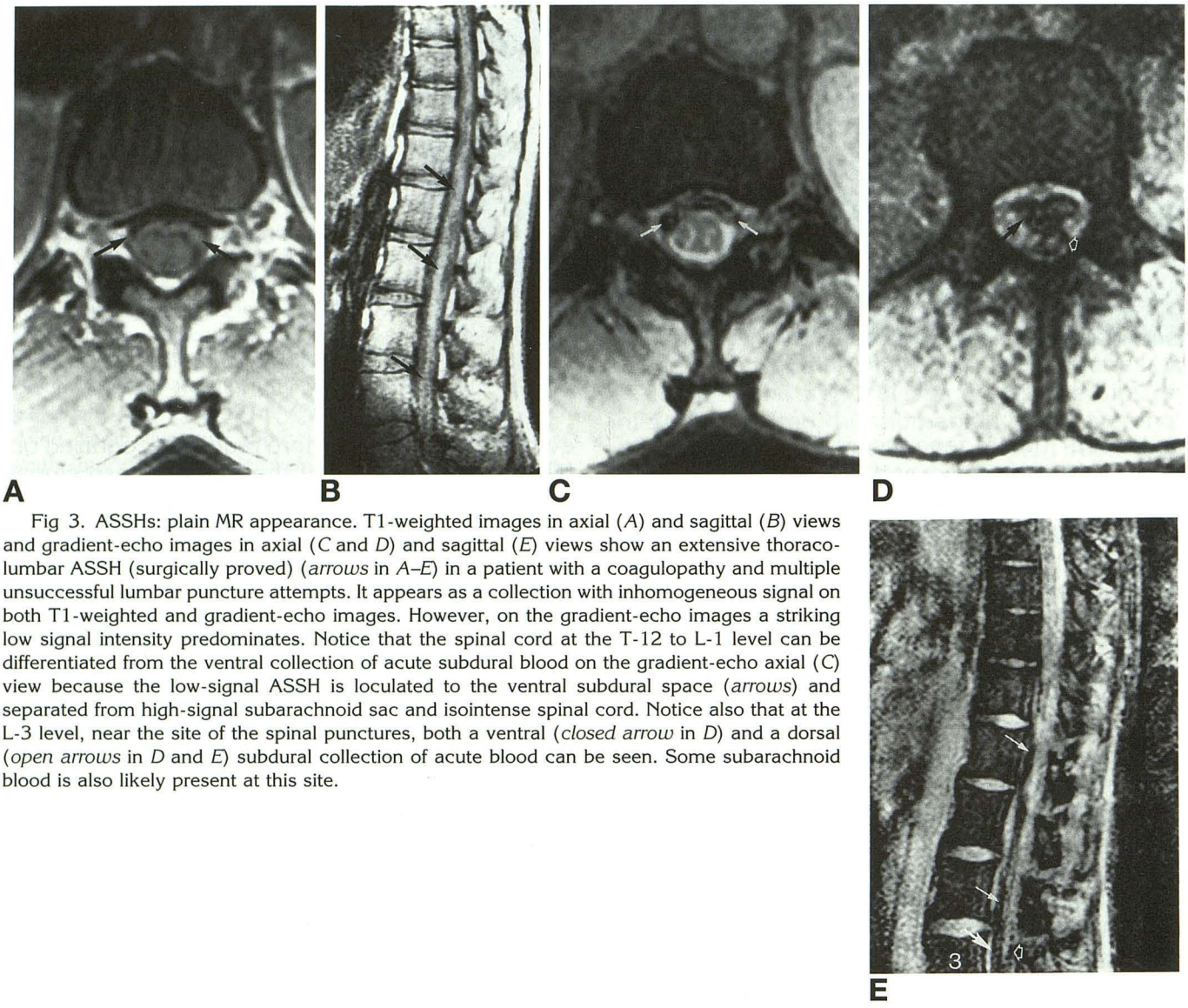

Fig 3. ASSHs: plain MR appearance. T1-weighted images in axial (*A*) and sagittal (*B*) views and gradient-echo images in axial (*C* and *D*) and sagittal (*E*) views show an extensive thoracolumbar ASSH (surgically proved) (*arrows* in *A–E*) in a patient with a coagulopathy and multiple unsuccessful lumbar puncture attempts. It appears as a collection with inhomogeneous signal on both T1-weighted and gradient-echo images. However, on the gradient-echo images a striking low signal intensity predominates. Notice that the spinal cord at the T-12 to L-1 level can be differentiated from the ventral collection of acute subdural blood on the gradient-echo axial (*C*) view because the low-signal ASSH is loculated to the ventral subdural space (*arrows*) and separated from high-signal subarachnoid sac and isointense spinal cord. Notice also that at the L-3 level, near the site of the spinal punctures, both a ventral (*closed arrow* in *D*) and a dorsal (*open arrows* in *D* and *E*) subdural collection of acute blood can be seen. Some subarachnoid blood is also likely present at this site.

Discussion

Hematomas in the spinal canal have long been recognized as lesions capable of producing sudden spinal cord and/or cauda equina compression (1–19). Their development has been related to a variety of different factors, including ruptured vascular malformations, underlying neoplasm, hypertension, coagulopathies, trauma, pregnancy, old age, infection, and spinal surgery (8, 13, 14, 30–32). Anticoagulant therapy, especially in combination with spinal punctures or epidural anesthesia, also has been regarded as an important predisposing factor (2, 6, 14, 33–35). In fact, anticoagulation initiated within 1 hour after a traumatic lumbar puncture and clotting studies greater than two times normal have been reported to increase the risk of bleeding (14, 33–35). Spinal hematomas, however, also have been described as occurring spontaneously or after only minor activities such as sneezing or coughing (13, 30–32, 36–39). Although usually acute (occurring within the first 48 hours of the event), some spinal hematomas have been identified as causes of chronic myelopathy (7, 31, 32, 39, 40). Because they rarely spontaneously remit (30), and because of their great propensity for causing severe irreversible neurologic deficits, immediate surgical evaluation of these compressive lesions has been strongly advocated (1, 9, 13, 15, 17).

Of the spinal hematomas, those in epidural locations are by far the most common, which

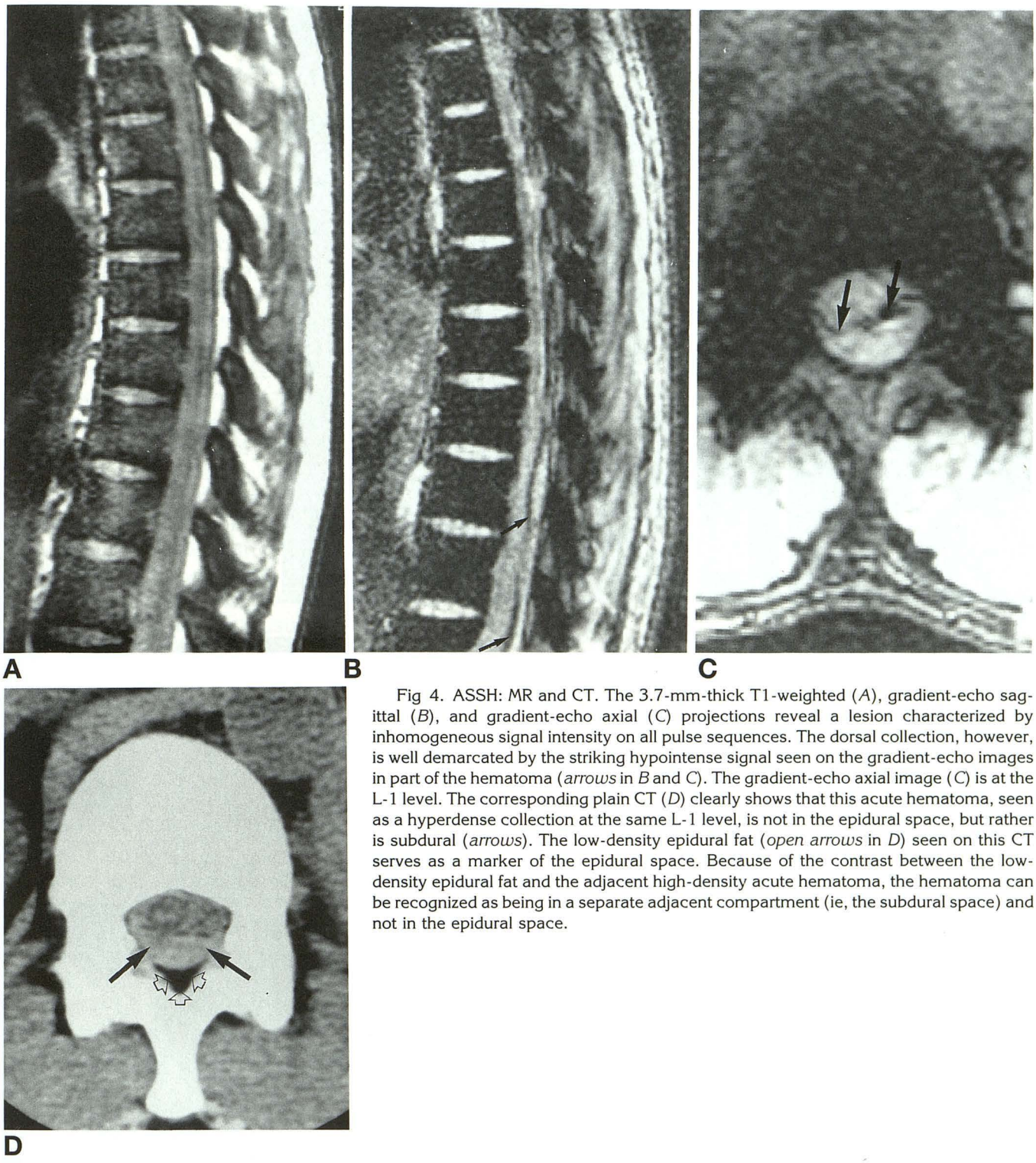

Fig 4. ASSH: MR and CT. The 3.7-mm-thick T1-weighted (*A*), gradient-echo sagittal (*B*), and gradient-echo axial (*C*) projections reveal a lesion characterized by inhomogeneous signal intensity on all pulse sequences. The dorsal collection, however, is well demarcated by the striking hypointense signal seen on the gradient-echo images in part of the hematoma (*arrows* in *B* and *C*). The gradient-echo axial image (*C*) is at the L-1 level. The corresponding plain CT (*D*) clearly shows that this acute hematoma, seen as a hyperdense collection at the same L-1 level, is not in the epidural space, but rather is subdural (*arrows*). The low-density epidural fat (*open arrows* in *D*) seen on this CT serves as a marker of the epidural space. Because of the contrast between the low-density epidural fat and the adjacent high-density acute hematoma, the hematoma can be recognized as being in a separate adjacent compartment (ie, the subdural space) and not in the epidural space.

explains why the clinical and radiologic manifestations of epidural hematomas have been the most often described (9, 11–33, 36, 37, 39, 40). It is important to recognize, however, that spinal hematomas also can occur in either subdural or subarachnoid locations and that these hematomas can cause neural compression comparable to that of an epidural hematoma (1–8, 34, 38, 41, 42). Because of the infrequent occurrence of spinal subdural hematoma and the even rarer occurrence of subarachnoid hematomas, their clinical features have been less commonly de-

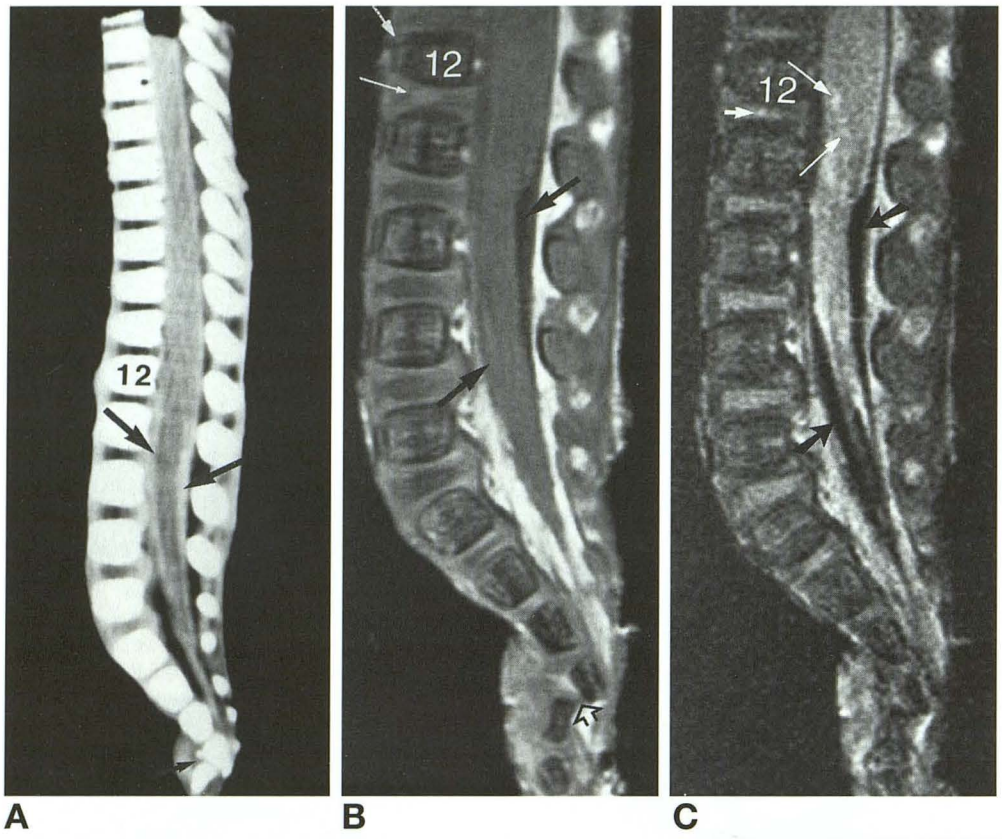

Fig 5. Postmortem case of ASSH.

A, Plain CT scan of the thoracolumbar spine with 1.5-mm-thick sections reveals a hyperdense collection of blood clearly within the dural sac (*large arrows*) and separate from the adjacent epidural low-density fat. A coccygeal fracture subluxation (*small arrow*) and a mild T-12 compression fracture are also seen.

B, The corresponding plain MR with a 3-mm-thick T1-weighted image in the sagittal view documents the subdural location of this acute spinal hematoma, showing it as an abnormal collection (*black arrows*) of isointense to hypointense signal within both the ventral and dorsal aspects of the spinal canal, clearly demarcated from the hyperintense epidural fat.

C, On the T2-weighted image in the sagittal view, the subdural blood is clearly distinguished from the epidural fat because of the striking hypointense signal to the ASSH (*black arrows*).

Also evident on the MR images in this infant who died from a shaking injury is the T-12 (*large white arrow* in *B*) and coccygeal (*open arrow* in *B*) fractures, and evidence of intervertebral disk and conus injury. Notice the hyperintense signal in the T-12 to L-1 disk space on T1- and T2-weighted images (*small white arrows* in *B* and *C*) and also the lack of normal configuration to the conus, within which there is abnormal hyperintense signal (*longer white arrows* in *C*). Notice also that the cerebrospinal fluid signal is not normal, and the cauda equina is difficult to distinguish because there is some blood in the subarachnoid space as well.

D, Cryomicrotome sections confirmed the large intrathecal hematoma (*arrow*), as well as the conus contusion, hemorrhagic contused disk, and the fractures. Also evident are small amounts of blood between the roots of the cauda equina.

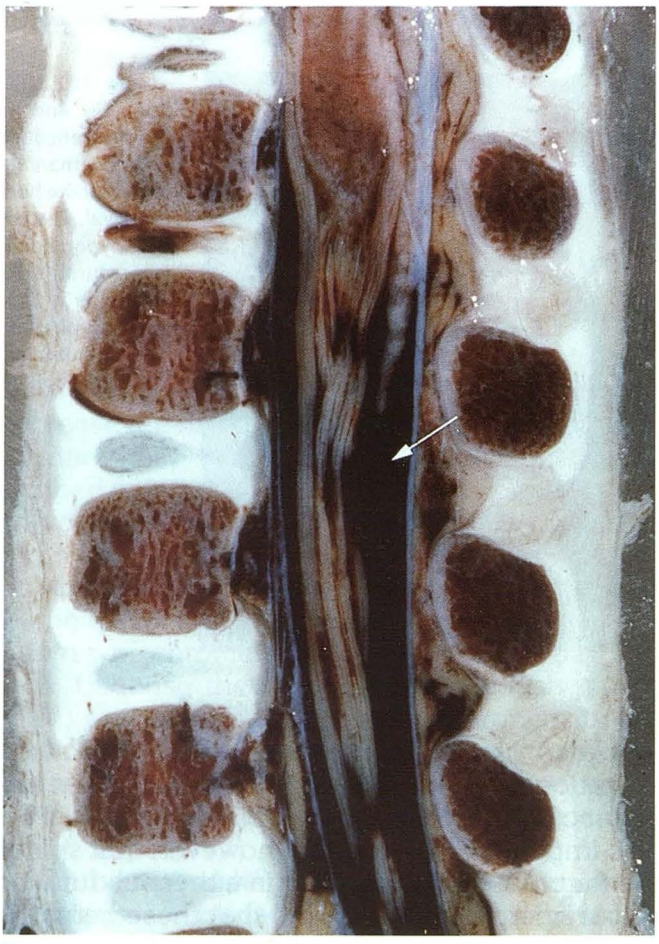

scribed, and their imaging characteristics have received little attention. Nevertheless, the need for correct compartmentalization of the hematoma has not been precluded by the less-common occurrence of the subdural and subarachnoid hematomas. Correct preoperative diagnostic location of the hematoma informs the surgeon of the need to open the dura or arachnoid to locate the hematoma, particularly in cases complicated by the coexistence of epidural and subdural hematomas.

The anatomy of the epidural, subdural, and subarachnoid spaces seems to be a predisposing factor to the development and extension of spinal hematomas. For example, the extensive network in the spine of thin-walled valveless epidural veins embedded in loose areolar tissue has been said to make rupture of these fragile, relatively unprotected vessels possible when they are subjected either to changes in intraabdominal and intrathoracic pressure or to injury from traumatic lumbar punctures (2, 13). Because the epidural space is largest posteriorly, the route of spread of these epidural hematomas is usually in the posterior epidural space (2, 13). In the cervical spine, the network of free or bridging epidural arteries that course from the nerve sheath to the arterial plexus on the spinal dura also has been viewed as an anatomically vulnerable site where epidural hematomas could form easily as a result of mechanical disruption (15). In contrast, subarachnoid hematomas do not readily develop, because of the pulsatile flow of cerebrospinal fluid that continuously occurs in this compartment. When bleeding does occur in the subarachnoid space, a hematoma usually does not form. Rather, the blood typically diffuses freely throughout the spinal subarachnoid pathway (1, 10). In the presence of an obstruction or very slow cerebrospinal fluid flow, however, the formation of a hematoma is favored (1).

The mechanism of hematoma formation in the spinal subdural space remains open to conjecture. However, an electron microscopy study by Haines et al recently offered explanations for subdural hematoma occurrence in the brain, which also seem plausible for the spine (43). According to these authors, the dura is composed externally of elongated flattened fibroblasts and large amounts of extracellular collagen; internally it is made up of flattened fibroblasts and extracellular spaces containing no extracellular collagen, with few cell junctions. Whereas the external layer of dura is strong, the inner dura or meningeal dura, also known as the dural border cell layer, is structurally weak and vulnerable to tearing open from injury (43). The adjacent arachnoid layer bears resemblance to the external dura in that it also is a strong barrier, being composed of larger cells with many cell junctions, no extracellular collagen, and no extracellular space. The numerous tight junctions in this layer prevent the free movement of fluids and ions. This arachnoid layer is further strengthened by the fact that arachnoid trabeculae formed from specialized fibroblasts attached to the inner arachnoid layer traverse the subarachnoid space and attach to the pia (43). According to Haines et al, under these anatomic conditions no potential space exists at the dura-arachnoid junction in the brain (43). Rather, the dural border cell layer, which is the structurally weakest point in the meninges, cleaves open when traumatic or other pathologic forces cause tissue injury (43). The space that is created in this fashion is actually within this distinct dural border cell layer as opposed to being in an anatomic subdural space (43). By common parlance, however, this pathologically or traumatically induced space is still usually referred to as the "subdural space" and has been so identified in this paper also.

Based on the anatomic observations of Haines et al (43), it is not difficult to imagine that in the spine the vulnerable inner dura, or dural border cell layer, also could be easily torn apart under certain circumstances, such as with multiple traumatic lumbar punctures in a patient with a preexisting coagulopathy. It is also easy to imagine that the hematoma could spread extensively in the spinal canal in this "cleaved open" space in the inner dura yet be confined between the tough external dura and arachnoid and thereby form a discrete mass.

An alternative hypothesis for the formation of spinal subdural hematomas could be offered based on the anatomic studies performed by others specifically in the spine (44, 45). Blomberg, for example, found that the spinal subdural space in 10 of 15 human autopsy cases opened easily with spinaloscopy (44). In his view, then, the spinal subdural space would be a potential space susceptible to injury during attempts at epidural anesthesia. A hematoma then could form easily in this subdural space.

Whether the spinal subdural hematomas described in our paper are within a cleaved-open inner dura or are actually in a true subdural space can only be determined by further anatomic investigations.

In the past, the diagnosis of spinal hematomas has been made based on a high degree of clinical suspicion and myelographic findings. The myelogram has been used to detect these obstructing lesions, to delineate their extent, and to indicate which particular compartment they involved (eg, epidural, subdural, and/or subarachnoid space) (8, 11–14, 31, 32). Because of the invasive nature of this procedure, and because this study is contraindicated in patients with coagulopathies, the role of myelography in identifying spinal hematomas gradually has diminished with the advent first of CT and then of MR.

Plain CT has been successfully used to diagnose acute spinal hematomas in the epidural space (1, 2, 13, 15, 20). These acute spinal epidural hematomas have been described on noncontrast CT scans as sharply demarcated hyperdense mass lesions of blood-equivalent density and of biconvex shapes that closely approximate the bony confines of the spinal canal, which displace and compress the less dense-appearing thecal sac and spinal cord (15, 20, 22–25, 40). They have been identified most commonly in a dorsolateral location (15, 20, 25, 40). On plain CT these acute spinal epidural hematomas have been differentiated from bleeding in the subarachnoid sac when the latter has been diffuse and seen as nonlocalized areas of increased density surrounding the more lucent-appearing spinal cord (20). The differentiation of acute spinal epidural hematomas on plain CT from acute spinal subdural hematomas has not been well described.

More recently, MR has been successfully used to diagnose acute spinal hematomas (26–29). On plain MR acute and subacute epidural hematomas have been reported to appear as well-demarcated biconvex collections with superiorly and inferiorly tapering margins, clearly separated from the spinal cord (28). Although often seen in dorsolateral locations (28), epidural hematomas also have been found on MR in ventral locations in the spinal canal, as those recently reported in the lumbar spine by Gundry and Heithoff, where they were seen in association with small concomitant disk herniations and underlying annular tears (29). A ventral location to an epidural hematoma also has been reported on MR in the midthoracic spine by Keane et al as a complication of acupuncture (21).

Because of the many advantages it offers, MR has been advocated as an imaging study well suited for the detection of spinal hematomas. Among the advantages of MR cited in the literature are its noninvasive nature, its superior contrast resolution to that of CT, and its ability to show directly the spinal cord and to survey quickly the entire spine to determine the extent of the spinal hematoma (21, 26–29). MR's sensitivity in detecting blood and its ability to specifically diagnose and stage hematomas have been emphasized (46–49). The ability of MR to show the breakdown products of blood has been most thoroughly described in the brain, and its value in the spine also has been recognized, particularly in patients with spinal cord injuries and intramedullary hemorrhages (26–29). The evolutionary changes that occur in intracranial hematomas have been thought applicable to spinal hematomas as well (26–29).

At 2 days of age on plain MR, spinal epidural hematomas have been reported by Rothfus et al to be isointense to hyperintense to spinal cord on T1-weighted images and hyperintense to spinal cord on T2-weighted images, whereas at 3 days of age, the hematoma has been described as an inhomogeneous hyperintense mass on T1-weighted images (28). At 10 days of age, epidural hematomas have been reported to be hyperintense on both T1- and T2-weighted images (21). Gundry and Heithoff, however, found a more variable appearance of epidural hematomas, encountering hyperintense signal on proton-density and T2-weighted images in only 30% of their cases (29). Their epidural hematomas, which usually could be distinguished from the lower–signal intensity adjacent disk herniation, ranged from intermediate to high signal intensity on both the proton-density and T2-weighted images (29). The time from clinical presentation to MR imaging in their series of 18 patients ranged from 2 to 870 days.

Although the MR appearance of blood in the epidural and intramedullary spaces has been described, the appearance of subdural blood has not been as clearly elucidated. In our study we found that MR could be used successfully to diagnose subdural hematomas in the spine. As opposed to acute epidural hematomas, which

were capped by epidural fat, the subdural hematomas were located within the thecal sac, separate from the adjacent extradural fat and separate from the adjacent osseous structures (Fig 2). In the subdural space, in contradistinction to the epidural space, the hematoma appeared clumped and loculated and was actually reminiscent of myelographic contrast in the subdural space from a subdural injection. With the patient in a supine position, ventrally located subdural blood did not gravitate to the dorsal aspect of the thecal sac and did not diffuse freely (Fig 3). The subdural blood, although often seen in a ventral location, was also observed posteriorly, laterally, and sometimes circumferentially. The signal characteristics of these subdural hematomas were similar to those previously reported for epidural hematomas and also to those already reported for acute and subacute hematomas in the brain. Of particular importance is the fact that on gradient-echo or T2-weighted images these acute spinal subdural collections had strikingly low signal intensity to a major portion of the collection because of the presence of deoxyhemoglobin, which allowed for the correct diagnosis of an acute subdural hematoma. Importantly, MR also could determine extent of a lesion and degree of cord and cauda equina compression.

We did encounter some diagnostic difficulties, however. When MR was interpreted without the corresponding CT and/or without pertinent clinical history, when the hematoma appeared inhomogeneous and of variable signal intensity, (depending on its exact age), and when there was blood present in other compartments (eg, epidural, subnarachnoid, and/or intramedullary), the MR picture was less clear (Fig 4). The signal of fat on gradient-echo or T2-weighted images also had a potential of being misinterpreted as blood in the adjoining epidural space. The ability of MR to discriminate subdural hematomas from hematomas in the subarachnoid space also remains to be determined. Nevertheless, despite these difficulties, we found that when plain CT and plain MR were used together, the diagnosis of a subdural hematoma could be made, and the need for myelography was obviated. CT was helpful in compartmentalizing the lesion, in confirming the presence of fresh blood, and in clearly differentiating the hyperdense subdural hematoma from the adjacent low-density fat.

Although we noted no striking differences in the imaging appearance of the spinal hematomas in our three hospitalized patients compared with our three postmortem formalin-fixed specimens, the potential for a disparity in results does exist and should be pointed out. Carvlin et al, for example, reported that after formalin fixation, the T1 and T2 values for white and gray matter in the cervical spinal cord of humans and rats were considerably reduced when imaged on an experimental 1.9-T MR system (50). In another article, one dealing with the T1 and T2 measurements over time in formalin-fixed human whole-brain specimens, Tovi and Ericsson also addressed the possibility of results being altered because of potential changes from the fixation process (51). They noted that formalin, a fixative that does not coagulate proteins, considerably alters the physical characteristics of tissue by binding itself in a cross-linking fashion to side groups of certain amino acids (51). They also noted that in formalin-fixed tissue a slight reduction of water content could be seen, and that the resultant mild dehydration of the tissue could result in reduced relaxation times (51). Nevertheless, they also noted that formalin fixation resulted in a gradual degradation of phospholipid structures, which they postulated might counteract to some degree the effect caused by the cross-linking, thereby resulting in a decrease in T1 in white matter after formalin fixation compared with gray matter (51). Furthermore, they pointed out that the postmortem MR appearance of cerebral tissue that had actually been reported previously in the literature seemed to have correlated well with the MR findings in vivo and with the histopathologic data (51).

Taking into account these reports concerning formalin-fixed specimens, it is certainly possible that in our study the decrease in the T2 relaxation values we saw in our acute spinal hematomas may have been accentuated by this formalin-fixation process. However, because striking hypointensity was also seen on gradient-echo or T2-weighted images in our hospitalized patients with ASSH, we feel that this potential difference in degree of T2 shortening did not affect our observations and conclusions. As for potential T1 shortening in our formalin-fixed specimens, we had no cases in which we saw bright signal on T1-weighted images in our postmortem specimens with ASSH.

We did not observe any differences in the imaging features of our three hospitalized patients with clotting disorders compared with our three postmortem subjects with no clotting disorders. One could postulate that the hematoma's extent and rapidity of formation might be affected by clotting factors. One also could argue that the degree of clotting and the amount of clot retraction may vary with the platelet concentration. However, in the work reported by Clark et al (52), fibrin polymerization and clot retraction had small effect on T2 at 1.5 T. The appearance of acute hematomas in vitro was not significantly altered by these factors at this high field strength (52, 53). Although many factors could have potentially shortened the T2 of acute hematomas at 1.5 T, including deoxygenation of blood, increase in hematocrit, and fibrin clot formation and retraction, the most important factor seemed to be deoxygenation, not fibrin clot formation and retraction (52). In our study, although we found no significant differences in the imaging appearance of acute spinal hematomas between our two groups, we acknowledge that the signal characteristics of hemorrhage are so complex that further experimental work in the spine might prove helpful in uncovering physiologic changes that might affect the imaging appearance of acute hematomas in the spine.

We conclude that plain CT and MR can be used as complementary studies if needed to establish the diagnosis of ASSH.

Acknowledgments

Gratitude is expressed to Jean Alli for secretarial assistance and to Chris Fletcher to photography.

References

1. Kirkpatrick D, Goodman SJ. Combined subarachnoid and subdural spinal hematoma following spinal puncture. *Surg Neurol* 1975;3:109–111
2. Edelson RN, Chernik NL, Posber JB. Spinal subdural hematomas complicating lumbar puncture: occurrence in thrombocytopenic patients. *Arch Neurol* 1974;31:134–137
3. Schiller F, Neligan G, Budtz-Olsen O. Surgery in haemophilia: a case of spinal subdural hematoma producing paraplegia. *Lancet* 1948;2:842–845
4. Wolcott GJ, Frunnet ML, Lahen ME. Spinal subdural hematoma producing paraplegia. *J Pediatr* 1970;77:1060–1062
5. Schaake T, Schafet ER. Spontaneous hemorrhage in the spinal canal. *J Neurol Neurosurg Psychiatry* 1970;33:715–716
6. Anagnostopoulos DI, Gortvai P. Spontaneous spinal subdural hematoma. *Br Med J* 1972;1:30
7. Stewart DH, Watkins ES. Spinal cord compression by chronic subdural hematoma. *J Neurosurg* 1969;31:80–82
8. Ainslie JP. Paraplegia due to spontaneous extradural or subdural hemorrhage. *Br J Surg* 1958;45:565–567
9. Packer NP, Cummins BH. Spontaneous epidural hemorrhage: a surgical emergency. *Lancet* 1978;1:356–358
10. De Angelis J. Hazards of subdural and epidural anesthesia during anticoagulant therapy: a case report and review. *Anesth Analg* 1972;51:676–679
11. Dawson BH. Paraplegia due to spinal epidural hematoma. *J Neurol Neurosurg Psychiatry* 1963;26:171–173
12. Cooper DW. Spontaneous spinal epidural hematoma. *J Neurosurg* 1976;26:343–345
13. Pear BL. Spinal epidural hematoma. *AJR Am J Roentgenol* 1972; 115:155–164
14. Alderman DB. Extradural spinal cord hematoma: report of a case due to dicumarol and review of the literature. *N Engl J Med* 1956;255:839–842
15. Beatty RM, Winston KR. Spontaneous cervical epidural hematoma: a consideration of etiology. *J Neurosurg* 1984;61:143–148
16. Lowrey JJ. Spinal epidural hematomas: experiences with three patients. *J Neurosurg* 1959;16:508–513
17. Grollmus J, Hoff J. Spontaneous epidural haemorrhage: good results after early treatment. *J Neurol Neurosurg Psychiatry* 1975; 38:89–90
18. Markham JW, Lynge HN, Stahlman GEB. The syndrome of spontaneous spinal epidural hematoma. *J Neurosurg* 1967;26:334–342
19. Harris ME. Spontaneous epidural spinal hemorrhage. *AJR Am J Roentgenol* 1969;105:383–385
20. Post MJD, Seminer PS, Quencer RM. CT diagnosis of spinal epidural hematoma. *AJNR Am J Neuroradiol* 1982;3:190–192
21. Keane JR, Ahmadi J, Gruen P. Spinal epidural hematoma with subarachnoid hemorrhage caused by acupuncture. *AJNR Am J Neuroradiol* 1993;14:365–366
22. Coin GC, Pennink M, Ahmad WD, Keranen VJ. Diving-type injury of the cervical spine: contribution of computed tomography to management. *J Comput Assist Tomogr* 1979;3:362–372
23. Zilkha A, Irwin GAL, Fagelman D. Computed tomography of spinal epidural hematoma. *AJNR Am J Neuroradiol* 1983; 4:1073–1076
24. Haykal HA, Wang AM, Zamani AA, Rumbaugh CL. Computed tomography of spontaneous acute cervical epidural hematoma. *J Comput Assist Tomogr* 1984;8:229–231
25. Laissy J-P, Milon P, Freger P, Hattab N, Creissard P, Thiebot J. Cervical epidural hematomas: CT diagnosis in two cases that resolved spontaneously. *AJNR Am J Neuroradiol* 1990;11:394–396
26. McArdle CB, Crofford MJ, Mirfakhraeem M, Amparo EG, Calhoun JS. Surface coil MR of spinal trauma: preliminary experience. *AJNR Am J Neuroradiol* 1986;7:885–893
27. Tarr RW, Drolshagen LF, Kerner TC, Allen JH, Partain CL, James AE Jr. MR imaging of recent spinal trauma. *J Comput Assist Tomogr* 1987;11:412–417
28. Rothfus WE, Chedid MK, Deeb ZL, Alba AA, Muroon JC, Sherman RL. MR imaging in diagnosis of spontaneous spinal epidural hematomas. *J Comput Assist Tomogr* 1987;11:851–854
29. Gundru CR, Heithoff KB. Epidural hematoma of the lumbar spine: 18 surgically confirmed cases. *Radiology* 1993;87:427–431
30. Harik SI, Raichle ME, Reis DJ. Spontaneously remitting spinal epidural hematoma in a patient on anticoagulants. *N Engl J Med* 1971;284:1355–1357
31. Boyd HR, Pear BL. Chronic spontaneous spinal epidural hematoma: report of two cases. *J Neurosurg* 1972;36:239–242

32. Hehman K, Norrell H. Massive chronic spinal epidural hematoma in a child. *Am J Dis Child* 1968;116:308–310
33. Senelick RC, Norwood CW, Cohen GH. "Painless" spinal epidural hematoma during anticoagulant therapy. *Neurology* 1976; 26: 213–215
34. Brem SS, Hafler DA, Van Llitert RL, Ruff RL, Reichert WH. Spinal subarachnoid hematoma: a hazard of lumbar puncture resulting in reversible paraplegia. *N Engl J Med* 1981;304:1020–1021
35. Ruff RL, Dougherty JH Jr. Evaluation of acute cerebral ischemia for anticoagulant therapy: computed tomography or lumbar puncture. *Neurology* 1981;31:736–740
36. Gold ME. Spontaneous spinal epidural hematoma. *Radiology* 1963;80:823–828
37. Tsai FY, Popp AJ, Waldman J. Spontaneous spinal epidural hematoma. *Neuroradiology* 1975;10:15–30
38. Slavin HB. Spontaneous intraspinal subarachnoid hemorrhage: report of a case. *J Nerv Ment Dis* 1937;86:425–427
39. Plotkin R, Ronthal M, Froman C. Spontaneous spinal subarachnoid hemorrhage: report of 3 cases. *J Neurosurg* 1966;25:443–446
40. Levitan LH, Wiens CW. Chronic lumbar extradural hematoma: CT findings. *Radiology* 1983;148:707–708
41. Masdeu JC, Breuer AC, Schoene WC. Spinal subarachnoid hematomas clue to a source of bleeding in traumatic lumbar puncture. *Neurology* 1979;29:872–876
42. Rengachary SS, Murphy D. Subarachnoid hematoma following lumbar puncture causing compression of the cauda equina. *J Neurosurg* 1974;41:252–254
43. Haines DE, Harkey HL, Al-Mefty O. The "subdural" space: a new look at an outdated concept. *Neurosurgery* 1993;32:111–120
44. Blomberg RG. The lumbar subdural extraarachnoid space of humans: an anatomical study using spinaloscopy in autopsy cases. *Anesth Analg* 1987;66:177–180
45. Nicholas DS, Weller RO. The fine anatomy of the human spinal meninges: a light and scanning electron microscopy study. *J Neurosurg* 1988;69:276–282
46. Edelman RR, Johnson K, Buxton R, et al. MR of hemorrhage: a new approach. *AJNR Am J Neuroradiol* 1986;7:751–756
47. Gomori JM, Grossman RI, Goldberg HJ, Zimmerman RA, Bilaniuk LT. Intracranial hematomas imaging by high field MR. *Radiology* 1985;157:87–93
48. Bradley WG Jr, Schmidt PG. Effect of methemoglobin formation on the appearance of subarachnoid hemorrhage. *Radiology* 1985;156:99–103
49. Fobben ES, Grossman RI, Atlas SW, et al. MR characteristics of subdural hematomas and hygromas at 1.5 T. *AJNR Am J Neuroradiol* 1989;10:687–693
50. Carvlin MJ, Asato R, Hackney DB, Kassab E, Joseph PM. High-resolution MR of the spinal cord in human and rats. *AJNR Am J Neuroradiol* 1989;10:13–17
51. Tovi M, Ericsson A. Measurements of T1 and T2 over time in formalin-fixed human whole-brain specimens. *Acta Radiol* 1992; 33:400–404
52. Clark RA, Watabane AT, Bradley WG, Roberts JD. Acute hematomas: effects of deoxygenation, hematocrit, and fibrin-clot formation and retraction on T2 shortening. *Radiology* 1990;175: 201–206
53. Thulborn KR, Atlas SW. Intracranial hemorrhage. In: Atlas SW, ed. *Magnetic Resonance Imaging of the Brain and Spine.* New York: Raven Press, 1991:175–221